

Manuscript Number: AJGS-D-10-00043

Title: The Kirsh gneiss dome: An extensional metamorphic core complex from the SE Arabian Shield.

Article Type: Original Paper

Abstract: Abstract

A number of gneiss-cored domes and antiforms are exposed along the regional strike-slip Najd fault system in the Arabian Shield and the eastern desert of Egypt. The mode of origin is still controversial although plausible comparisons with modern metamorphic-core complexes were made in some well-studied areas. The Kirsh dome is located within the major Ar Rika shear zone and consists of a core of orthogneiss /migmatite and an envelope of paragneisses with locally-abundant kyanite-bearing quartzites. The dome is surrounded by the low-grade metasediments of the Murdama Group, and is bound from the south by a low-angle dip-slip fault. Beyond the southern strand of the Ar Rika fault is the Kibdi Basin which hosts unmetamorphosed sediments belonging to the Jibalah Group; this group occupies scattered pull-apart basins closely associated with releasing bends along the Najd fault system. Little dating was done on the gneiss domes of the Arabian Shield; however, recent dates from similar structures in the eastern desert and Sinai range from 580 to 620 Ma. A similar, albeit younger $^{40}\text{Ar}/^{39}\text{Ar}$ age of 557 ± 15 Ma was obtained from a biotite paragneiss south of Jabal Kirsh; this age difference probably represent the time interval it took the Kirsh rocks to cool below the biotite closures temperature and would place a lower age limit for the dome. The Kirsh dome occupies an extensional zone between left-stepping faults; movement within this zone might have caused enough decompression to trigger fluid-absent melting in the middle crust especially as the rocks cross the biotite dehydration solidus. Diapiric ascent aided by strike slip dilatancy pumping led to the emplacement of the Kirsh rocks in their present position within the Murdama Group metasediments. Keywords: Arabian Shield; gneiss dome; core complex; Najd fault system.

The Kirsh gneiss dome: An extensional metamorphic core complex from the SE Arabian Shield.

Ahmad M. Al-Saleh

Geology Department, King Saud University, Riyadh, Saudi Arabia.

Abstract

A number of gneiss-cored domes and antiforms are exposed along the regional strike-slip Najd fault system in the Arabian Shield and the eastern desert of Egypt. The mode of origin is still controversial although plausible comparisons with modern metamorphic-core complexes were made in some well-studied areas. The Kirsh dome is located within the major Ar Rika shear zone and consists of a core of orthogneiss /migmatite and an envelope of paragneisses with locally-abundant kyanite-bearing quartzites. The dome is surrounded by the low-grade metasediments of the Murdama Group, and is bound from the south by a low-angle dip-slip fault. Beyond the southern strand of the Ar Rika fault is the Kibdi Basin which hosts unmetamorphosed sediments belonging to the Jibalah Group; this group occupies scattered pull-apart basins closely associated with releasing bends along the Najd fault system. Little dating was done on the gneiss domes of the Arabian Shield; however, recent dates from similar structures in the eastern desert and Sinai range from 580 to 620 Ma. A similar, albeit younger $^{40}\text{Ar}/^{39}\text{Ar}$ age of 557 ± 15 Ma was obtained from a biotite paragneiss south of Jabal Kirsh; this age difference probably represent the time interval it took the Kirsh rocks to cool below the biotite closures temperature and would place a lower age limit for the dome. The Kirsh dome occupies an extensional zone between left-stepping faults; movement within this zone might have caused enough decompression to trigger fluid-absent melting in the middle crust especially as the rocks cross the biotite dehydration solidus. Diapiric ascent aided by strike slip

1 dilatancy pumping led to the emplacement of the Kirsh rocks in their present position
2 within the Murdama Group metasediments.
3

4 Keywords: Arabian Shield; gneiss dome; core complex; Najd fault system.
5
6

7
8 Gneiss domes were identified from most of the terranes of the
9 Arabian-Nubian Shield and especially from the intervening sutures where
10 they had conventionally been ascribed to the compressional stresses that
11 accompanied terrane amalgamation (Schmidt *et al*, 1979). More recently,
12 many of these structures were re-interpreted as metamorphic core
13 complexes similar to those of the North American Cordillera and as such
14 were taken to represent a stage of crustal extension concomitant with
15 orogenic collapse (e.g. Brooijmans *et al*, 2003), although other viable
16 models such as fold interference patterns and folded nappes were
17 proposed (Fowler *et al*, 2007; Fowler and El-Kalioubi, 2002). The
18 difference between gneiss domes and core complexes has been blurred in
19 recent years owing to the fact that many author tend to take the two terms
20 as being synonymous. Some metamorphic core complexes are indeed
21 domes or contain gneiss domes within them (Whitney *et al*, 2004), but
22 not all gneiss domes posses the essential elements of a true metamorphic
23 core complex. A core complex consists of a metamorphic interior and an
24 unmetamorphosed (or slightly metamorphosed) cover separated by a
25 mylonitic decollement along a low-angle normal fault (detachment fault).
26
27
28
29
30
31
32
33
34
35
36
37
38
39
40
41
42
43
44
45
46
47
48
49
50
51
52
53
54
55
56
57
58
59
60
61
62
63
64
65

1 The structures are often dome-like with the major fold axis parallel to the
2 regional extension (Yin, 1991).
3
4

5 The Arabian-Nubian Shield marks the northern collision zone
6 between East and West Gondwana, a process that began at *c.* 870 Ma
7 with the breakup of Rodinia and the formation of island arcs within the
8 Mozambique Ocean, which were later amalgamated during collision to
9 form the terranes of the Arabian-Nubian Shield; orogenic activity ceased
10 and a passive margin formed at *c.* 550 Ma (Johnson and Woldehaimanot,
11 2003). Al-Saleh *et al* (1998) suggested that oblique convergence induced
12 a major transpressional orogeny that affected the eastern half of the
13 Arabian Shield culminating at *c.* 600 Ma, and was probably followed by
14 major movement along the Najd sinistral strike-slip System.
15 Transpression is an efficient mechanism in crustal thickening and if
16 accompanied by transcurrent movement then it would be a favorable
17 milieu for the generation of migmatites and anatectic granites (D'Lemos
18 *et al*, 1992). It is generally accepted that tectonism in the Arabian shield
19 has changed from convergence to extension after 600 Ma (Genna *et al*,
20 2002); a manifestation of which is an inferred widespread unroofing
21 induced by low-angle detachment faults resulting eventually in the
22 exhumation of mid-crustal segments in metamorphic core complexes akin
23 to those of the Basin and Range province of the North American
24 Cordillera (e.g. Blasband *et al*, 2000). Although the deeper erosion level
25
26
27
28
29
30
31
32
33
34
35
36
37
38
39
40
41
42
43
44
45
46
47
48
49
50
51
52
53
54
55
56
57
58
59
60
61
62
63
64
65

1 of the Arabian Shield precludes direct comparison with assumed modern
2 analogues, it is still nevertheless possible to notice some similarities in
3 deformational style especially in the vicinity of major crustal-scale
4 structures.
5
6
7
8
9

10
11 Among the most interesting domal-structures in the Southeastern
12 Arabian Shield is the Jabal Kirsh gneissic antiform and its enveloping
13 mantle of kyanite-bearing metavolcanics (Delfour, 1979), which are
14 exposed along a segment of the Ar Rika sinistral strike-slip fault, one of
15 the major lineaments of the regional Najd Fault System (Johnson and
16 Kattan, 1998).
17
18
19
20
21
22
23
24
25
26

27 **Regional Geology:**

28
29 The study area is located close to the southeastern periphery of the
30 Arabian shield (Fig-1), and is underlain by Late Proterozoic layered rocks
31 and intrusives belonging to the Afif Composite Terrane (Stoeser and
32 Stacey, 1988; Johnson, 1998). The main structural feature is the Ar Rika
33 Fault which extends for more than 1000 km from the southeastern
34 boundary of the shield to the northern Red Sea coast and possibly into the
35 Sinai Peninsula. For much of its length, the Ar Rika Fault displays a
36 brittle-ductile nature with numerous exposures of gneissic belts most
37 conspicuous among them are the Kirsh granitic gneisses, as well as the
38 Qazaz, Wajiyah and Hamadat domes further north (Nehlig *et al*, 2001).
39
40
41
42
43
44
45
46
47
48
49
50
51
52
53
54
55
56
57
58
59
60
61
62
63
64
65

1 (Genna *et al*, 2002) that may reflect different modes of origin. The Kirsh
2 dome is unique in having extensive outcrops of kyanite-bearing
3 quartzites, signifying uplift of high-pressure mid-crustal material. On the
4
5
6
7
8
9
10
11
12
13
14
15
16
17
18
19
20
21
22
23
24
25
26
27
28
29
30
31
32
33
34
35
36
37
38
39
40
41
42
43
44
45
46
47
48
49
50
51
52
53
54
55
56
57
58
59
60
61
62
63
64
65

(Genna *et al*, 2002) that may reflect different modes of origin. The Kirsh dome is unique in having extensive outcrops of kyanite-bearing quartzites, signifying uplift of high-pressure mid-crustal material. On the decompensative isostatic residual gravity map of Mogren *et al* (2008) the Ar Rika fault zone is characterized by broad positive gravity anomalies (20–30 mGal), which they consider as the signature of a deep-lying high density gneissic mass.

20 In the study area, the Ar Rika Fault is bound to the northeast by the
21
22
23
24
25
26
27
28
29
30
31
32
33
34
35
36
37
38
39
40
41
42
43
44
45
46
47
48
49
50
51
52
53
54
55
56
57
58
59
60
61
62
63
64
65

In the study area, the Ar Rika Fault is bound to the northeast by the molassic sediments of the Murdama Group, while a heterogeneous assemblage of metavolcanics and intrusives is exposed on the opposite side; beyond which is the extensive Dahul gneissic terrain (Ramsay *et al*, 1984), an extensive structural/lithologic province made up of migmatites, granitic gneisses as well as syn- and post-tectonic granites. Further south the fault cuts through the Murdama rocks and its associated granites for a distance of about 120 km to the SE edge of the Shield where it is covered by Paleozoic sediments. To the north it cuts through various units and sutures and hosts a number of pull-apart basins infilled with the unmetamorphosed sediments and volcanics of the Jibalah Group.

51 According to geologic map of the Wadi ar Rika Quadrangle
52
53
54
55
56
57
58
59
60
61
62
63
64
65

According to geologic map of the Wadi ar Rika Quadrangle (Delfour, 1980), the Kirsh Dome is an anticlinorium cored by the Hawriyah orthogneiss which he interprets as an elliptical syntectonic intrusion of biotite granite emplaced within amphibolite-grade leptites

1 and amphibolites; this metamorphic envelope is referred to by Delfour
2 (1980) as the Mahadib Belt, which he considers to be derived from
3 volcanic rocks and sediments attributed to the Hulayfah Group of the
4
5 Nuqrah area in the northern shield on the basis of lithological and
6
7 assumed age similarity. Along the contacts, the granitic gneisses are
8
9 strongly foliated and possess the same shallow-plunging lineations of the
10
11 host metamorphites; the contact between these two units is gradational
12
13 with thick concordant sheets of granite injected into the metamorphic
14
15 rocks; towards the central part of the intrusion, foliation is less
16
17 pronounced, yet enclaves of country rocks are still common.
18
19
20
21
22
23
24
25
26
27

28 The granitic core and its surrounding metamorphic assemblage
29 were designated by Johnson (2003) as orthogneiss and paragneiss
30 respectively and the whole suite was referred to as the Kirsh gneiss belt.
31
32 Both segments appear on the compiled 1:1,500,000 map of the Arabian
33
34 Shield as one unit of “unassigned schist and gneiss” not included within
35
36 any of the stratigraphic groups of the shield (Johnson, 2006a); this
37
38 description applies to other metamorphic suites associated with Najd
39
40 faults. The igneous core was described by Johnson and Woldehaimanot
41
42 (2003) as a strongly foliated biotite monzogranite orthogneiss (Al
43
44 Hawriyah Anticlinorium) intruded into steeply dipping kyanite-quartz
45
46 schist at the southeastern end of the Ar Rika-Qazaz Shear System. On the
47
48 presumption that the Al Khushaymiyah complex to the NE, which is
49
50
51
52
53
54
55
56
57
58
59
60
61
62
63
64
65

1 composed of massive monzogranite, is an undeformed equivalent of the
2
3 Hawriyah orthogneiss, they assumed that activity on this section of the Ar
4
5 Rika Shear Zone is dated at c. 610Ma.
6

7
8
9 The detailed geologic setting of the Kirsh Dome is clearly a matter
10
11 of debate; however, there is a general agreement on the igneous intrusive
12
13 nature of its core and the presence of volcanosedimentary protoliths in the
14
15 metamorphic mantle; the latter is believed to have been originally made
16
17 up of felsic and siliceous tuffs grading to chert with andesitic pyroclastics
18
19 and graywackes on the basis of correlation with the Hulayfah Group
20
21 (Collenette and Grainger, 1994). Nevertheless, it seems improbable that
22
23 the rocks of the Kirsh area are an extension of the Hulayfah Group
24
25 because of the great distance from, lack of mapped continuity with, and
26
27 inferred different tectonic settings between the Wadi ar Rika and Nuqrah
28
29 areas (Johnson, 2006b); it is more likely that they are the high-grade
30
31 equivalents of the adjacent Siham Group (Agar, 1985), or the Rika
32
33 Formation (Johnson, 2005) which is located only 15 km from the
34
35 southern extension of the Ar Rika Fault and has a volcanosedimentary
36
37 assemblage metamorphosed in the greenschist facies.
38
39
40
41
42
43
44
45
46
47
48
49
50

51 Further east from the Kirsh Dome is a similar structure known as
52
53 the Artawi Structural Window (ASW) which is basically a migmatite
54
55 dome emplaced within the easternmost major strand of the Najd System
56
57 (Fig-1), and which is believed to be coeval with movement along the
58
59
60
61

1 Rika Fault (Al-Saleh *et al*, 1998). The ASW is dominated by basic
2
3 migmatites and high-grade biotite and garnet–biotite paraschists admixed
4
5 with granites from the heterogeneous Abu Isnun pluton which range in
6
7 composition from pyroxene diorites and tonalites to porphyritic alkali-
8
9 feldspar granites
10

11 **Local Geology:**

12
13
14 The northern tip of the Kirsh Dome was the main focus of field
15
16 work in this study (Fig-2) due mainly to its excellent outcrops of the
17
18 different lithologies that make up the dome and also because it has
19
20 extensive outcrops of kyanite-bearing quartzites that are unique in the
21
22 Arabian Shield, and may have important implications for the evolution of
23
24 this domal structure. The physiography of the region is dominated by the
25
26 Jabal Kirsh inselberg, a 1300 m-high massif of biotite paragneiss that
27
28 marks the northern end of the Kirsh Dome. The main strand of the Ar
29
30 Rika Fault runs about 20 km southwest of Jabal Kirsh, and has many
31
32 exposures of well-developed ultramylonite.
33
34
35
36
37
38
39
40
41
42
43
44

45 Scattered outcrops of kyanite-bearing quartzite are located about 7
46
47 km west of Jabal Kirsh in a 15 km long belt that contains layers of
48
49 quartzite with up to 20% of white kyanite. On the basis of relict textures,
50
51 the protolith of these quartzites is believed to be an alumina-rich rhyolite
52
53 rather than a metapelite (Delfour, 1980). East of the dome are the
54
55 extensive molassic sediments of the Murdama Group which are mainly
56
57
58
59
60
61
62
63
64
65

1
2
3
4
5
6
7
8
9
10
11
12
13
14
15
16
17
18
19
20
21
22
23
24
25
26
27
28
29
30
31
32
33
34
35
36
37
38
39
40
41
42
43
44
45
46
47
48
49
50
51
52
53
54
55
56
57
58
59
60
61
62
63
64
65

greywackes and conglomerates belonging to the Zaydi Formation and showing the effect of contact metamorphism up to amphibolite facies conditions. Mineral and grain lineations are well-developed in the Murdama rocks all along the contact and are mainly concordant with those of the adjacent dome rocks. Beyond the main Rika Fault are the unmetamorphosed clastic sediments of the Jibalah Group, occupying a wedge-shaped half graben known as the Kibdi Basin. These sediments are associated with Najd faulting throughout the central and northern shield, and the Kibdi Basin is the southernmost exposure of the group; they are believed to occupy pull-apart basins formed at the releasing bends of the Najd system (Matsah, 2000). A thin sliver of Murdama rocks separates the Jibalah sediments from the dome; the contact of this segment of the Murdama with the Kirsh gneisses is marked by a 50 km long thrust fault according to the map of Delfour (1980).

40
41
42
43
44
45
46
47
48
49
50
51
52
53
54
55
56
57
58
59
60
61
62
63
64
65

Inside the dome most of the rocks are metamorphosed to the amphibolite facies with the intensity of metamorphism increasing towards the center. The rock types are mainly gneissic with minor metabasites and quartzofeldspathic lithologies; abundant streaks of mylonite delineating minor shear zones run roughly parallel to the main segment of the Ar Rika Fault. Most rocks are foliated and some exhibit well-developed mineral lineations defined by hornblende, kyanite and mafic lenses. Delfour (1980) identifies two phases of folding, the first of which (F_1)

1 was coeval with amphibolite grade metamorphism and induced an axial-
2
3 plane cleavage and NW plunging lineations. The second phase (F₂) is a
4
5 post-metamorphic event and is less conspicuous; it affected mainly the
6
7 Murdama sediments through flexuring perpendicular to F₁ and produced
8
9 a noticeable crenulation cleavage in pelitic beds.
10

14 **Structural Geology and Geochronology:**

16
17 Observations during the field work of this study are in general
18
19 agreement with the findings of Delfour (1979, 1980) and Genna *et al*
20
21 (2002) as regards rock types and structures. Foliation with a strike
22
23 generally parallel to the long axis of the dome and moderate to steep dips
24
25 (45-90°) is generally well-developed especially in the paragneisses.
26
27 Mineral and grain lineations have a general NW trend and shallow to
28
29 moderate plunge (Fig-3). It was suggested by Johnson and
30
31 Woldehaimanot (2003) that the gentle plunge of the northwesterly
32
33 trending mineral and elongate-pebble lineations indicates a large
34
35 component of constriction, or unidirectional stretching. Similar structural
36
37 relations are to be found in metamorphic core complexes in the eastern
38
39 desert of Egypt lying roughly on the same Rika lineament (e.g. Fritz *et al*,
40
41 1996; Loizenbauer *et al*, 2001). According to the structural model of
42
43 Genna *et al* (2002) the Kirsh kyanite-bearing quartzites represent the
44
45 exhumation of a deep metamorphic facies within a domain of
46
47 transpressive ductile deformation; the extent of vertical uplift induced by
48
49
50
51
52
53
54
55
56
57
58
59
60
61
62
63
64
65

1 transpression was estimated to be about 10 to 15 km on the basis of the
2
3 metamorphic assemblage of the Kirsh dome (Nehlig *et al*, 2002).
4

5 The fact that gneiss domes in the Arabian-Nubian are in many
6 cases associated with crustal-scale transcurrent fault systems is highly
7 suggestive of a genetic role as relates to emplacement and possibly
8 magma genesis. Much work has been carried out in the past two decades
9 on the gneiss domes of Sinai and the eastern desert of Egypt, and their
10 relationships with presumed extensions of the Najd faults (Fritz *et al*,
11 2002; Abd El-Wahed, 2008), and there is a general agreement on the
12 causative role of sinistral strike-slip movement in the exhumation of core
13 complexes with varying tectonic scenarios and timing. Most models
14 envisage some form of extension (Brooijmans *et al*, 2003; Fritz *et al*,
15 2002; Fowler and Hassan, 2008) accompanied by the formation of
16 peripheral pull-apart basins infilled with the sediments of the Hammamat
17 Group (Abd El-Wahed, in press; Shalaby *et al*, 2006). A zone of intense
18 high-temperature mylonite that separates a brittle attenuated upper crust
19 from a deep exhumed crust in the Sibai domal structure was recognized
20 by Abd El-Wahed (2008); he concludes that the existence of sub-
21 horizontal lineation, sub-vertical foliation, strike-slip shear zones and the
22 pull-apart Atawi basin supports the idea of wrench-dominated
23 transpression and regional extension during formation and exhumation of
24 the Sibai core complex.
25
26
27
28
29
30
31
32
33
34
35
36
37
38
39
40
41
42
43
44
45
46
47
48
49
50
51
52
53
54
55
56
57
58
59
60
61
62
63
64
65

1 Age determinations from gneissic antiforms and belts in the eastern
2
3 desert of Egypt lie mainly within the late stages of cratonization of the
4
5 Arabian-Nubian Shield, with a clear clustering of ages in the period 620-
6
7 580 Ma (Fritz *et al*, 1996; Fritz *et al*, 2002; Andresen *et al*, 2009;
8
9 Loizenbauer, 2001; Eliwa, 2008). Recent evidence utilizing SHRIMP U-
10
11 Pb on zircons revealed that the time interval 579-594 Ma was the main
12
13 period for the generation of extension-related monzogranites,
14
15 syenogranites and alkali granites in Sinai (Ali *et al*, 2009). However,
16
17 there is a noticeable dearth of chronological data from Arabian Shield
18
19 gneissic terrains, especially as relates to their metamorphic/exhumation
20
21 ages. The only well-constrained emplacement ages for a granite-
22
23 migmatite dome in the eastern Arabian Shield are two $^{40}\text{Ar}/^{39}\text{Ar}$ dates
24
25 from the migmatitic metabasites and garnet-biotite schists of the Artawi
26
27 Structural Window which are concentrated around 600 Ma (Al-Saleh *et*
28
29 *al*, 1998).

30
31
32
33
34
35
36
37
38
39
40
41
42
43 In order to obtain an age estimate of the uplift of the Kirsh
44
45 gneisses, a sample of biotite paragneiss was collected from the southern
46
47 exposure of Jabal Kirsh and a biotite concentrate was prepared and
48
49 irradiated for age determination using the step-heating $^{40}\text{Ar}/^{39}\text{Ar}$
50
51 technique. Analysis was carried out at the Department of Earth Sciences,
52
53 Liverpool University. The mica separate, purified using an isodynamic
54
55 separator, was sealed in a quartz vial which was packed in a 150 mm
56
57
58
59
60
61
62
63
64
65

1
2
3
4
5
6
7
8
9
10
11
12
13
14
15
16
17
18
19
20
21
22
23
24
25
26
27
28
29
30
31
32
33
34
35
36
37
38
39
40
41
42
43
44
45
46
47
48
49
50
51
52
53
54
55
56
57
58
59
60
61
62
63
64
65

canister and irradiated with a neutron flux of $2 \times 10^{20} \text{ mm}^{-2}$ in the Petten reactor, Holland. Cadmium shielding was used to reduce the thermal neutron flux, and flux gradients were monitored with the MMhb-1 standard using an age of 520.4 Ma. The irradiated sample was placed in degassed molybdenum crucible, heated for 30 minutes for each step, and the released gases were purified using getters and liquid N₂ cold fingers. Argon isotope composition was measured with a modified AEI MS10 mass spectrometer with a 0.45-T magnet and automatic scanning. The errors are quoted at the 95% confidence level.

The gas was released in 13 heating steps giving a total gas age of 458 ± 1.1 Ma; steps 2-10 were chosen for age calculations and they contained 62% of the ³⁹Ar. Since such deep seated rocks commonly display non-atmospheric initial ⁴⁰Ar/³⁶Ar ratios, isochron ages are preferred to plateau ages because they need no prior assumption regarding initial Ar composition. On the ⁴⁰Ar/³⁶Ar vs. ³⁹Ar/³⁶Ar isochron diagram (Figure-4), the points yield a robust linear array with a mean squared weighted deviate (MSWD) value of 1.73, and an age of 557 ± 15 Ma. This age estimate is coeval with the nearby Dahul gneisses from which ages of 535-599 Ma were determined (Kroner *et al*, 1979 and references therein), but slightly younger than the above quoted dates from Egyptian complexes, due probably to the low closure temperature of biotite (c.300 °C) for argon (Hodges, 1991); this date should therefore be

1 considered as a cooling rather than an emplacement age, and would serve
2 as a minimum age for the development of the Kirsh structure.
3
4

5 The age of the Jibalah basins and the equivalent Hammamat Group
6 of Egypt has a direct bearing on the age of the Najd faults and associated
7 gneisses, yet direct determinations are hampered by the lack of rock types
8 suitable for isotopic measurements and hence most age estimates of these
9 sediments are based on cross-cutting relationships with igneous
10 lithologies. A 576 ± 5 Ma U–Pb zircon crystallization date from a felsite
11 dyke that cuts the Al Jifn basin (Matsah and Kusky, 2001) constrains the
12 lower age limit of the Jibalah in the north-central shield. Miller *et al*
13 (2008) obtained concordant SHRIMP ages as young as 599 ± 4.8 (core)
14 and 570 ± 4.6 (rim) from detrital zircons extracted from a diamictite
15 interval in the Dhaiqa Basin which lies within a putative extension of the
16 Rika Fault. Granitic basement in the Jabal Jibalah type area yields a Rb–
17 Sr whole-rock age of 574 ± 28 Ma (Calvez *et al.*, 1983), and K–Ar ages
18 of 567 ± 6 and 581 ± 7 Ma were reported by Brown *et al* (1989) from
19 volcanic horizons in basins from the central shield. Available age
20 estimates as well as field relations and overall geologic setting led
21 Johnson (2003) to conclude that the deposition of the Jibalah Group took
22 place mainly in the time interval 580–570 Ma. In Egypt, SHRIMP dates
23 from detrital zircons collected from the basal part of the Hammamat
24 Group are as young as 585 ± 13 Ma (Wilde and Youssef, 2002); previous
25
26
27
28
29
30
31
32
33
34
35
36
37
38
39
40
41
42
43
44
45
46
47
48
49
50
51
52
53
54
55
56
57
58
59
60
61
62
63
64
65

1 estimates include a zircon ‘model’ age of 583 Ma for a cross-cutting
2 granite (Stern & Hedge 1985), and a 585 ± 15 Ma Rb-Sr whole-rock age
3 from the sediments of Gebel Dokhan (Willis *et al*, 1988).
4
5
6

7 **Exhumation of the Kirsh Dome:** 8 9

10 It is evident from field relations and the various age estimates that
11 many gneiss domes in the Arabian-Nubian Shield have developed in a
12 close association with Najd faulting following terrane amalgamation and
13 cratonization, and most of those in the eastern Egyptian desert and Sinai
14 have been interpreted as metamorphic core complexes. The classic model
15 of core complex exhumation requires the presence of a low angle normal
16 fault (detachment fault) to induce unroofing and initiate crustal flow and
17 isostatic uplift, with no melting or plutonism required. However, in the
18 case of the Kirsh Dome it is necessary to explain the origin of the
19 Hawriyah granite and provide a viable mechanism for its emplacement.
20 Melting of crustal rocks is viewed as an essential part of gneiss dome
21 development (Teyssier and Whitney, 2002); therefore most domes are in
22 fact anatectic migmatite domes, and this is borne out by the fact that
23 many Precambrian domes in particular are dominated by granitic plutons
24 (Whitney *et al*, 2004).
25
26
27
28
29
30
31
32
33
34
35
36
37
38
39
40
41
42
43
44
45
46
47
48
49
50
51
52
53

54 Johnson and Woldehaimanot (2003) describe the Hawriyah
55 monzogranite as being located in a zone of extension between left-
56 stepping faults along the sinistral Ar Rika Fault Zone. The presence of the
57
58
59
60
61
62
63
64
65

1 Kibdi pull-apart basin indicates a releasing bend along the Rika Fault in
2
3 the Kirsh area, it is suggested here that extension concomitant with such
4
5 movement could have caused enough decompression to trigger
6
7 substantial partial melting in the middle or even lower crust which
8
9 generated a buoyant granitic diapir. Such a process would have been
10
11 greatly assisted by the development of a detachment fault leading to rapid
12
13 exhumation and near-isothermal decompression. The Najd fault system in
14
15 the eastern desert of Egypt is associated with low-angle normal faults
16
17 marking the northern and southern boundaries of metamorphic complexes
18
19 and forming extensional bridges between them (Fritz *et al*, 1996); it is
20
21 believed that the combined effect of strike-slip and normal faulting led to
22
23 the rapid late stage exhumation of the Meatiq and Hafafit domes and
24
25 continued to c. 580 Ma (Fritz *et al*, 2002).
26
27
28
29
30
31
32
33
34
35
36

37 It was noted by Johnson (2000) that southwest-directed extension
38
39 and normal dip slip characterized later movement on the Ar Rika shear
40
41 zone. The lineament defining the western boundary of the Kirsh dome
42
43 and identified by Delfour (1980) as a thrust is an excellent candidate for
44
45 the role of a detachment fault since it has the necessary strike direction
46
47 and a low dip angle; more importantly, it is inconceivable how a slice of
48
49 the Murdama molasses could have been transported westward from the
50
51 main Murdama basin along a an easterly moving thrust; this thrust is
52
53 clearly going the wrong way, and despite the lack of proper kinematic
54
55
56
57
58
59
60
61
62
63
64
65

1 indicators to establish the sense of slip, a more plausible explanation for
2
3 the existence of the Murdama sliver west of the dome is that a low-angle
4
5 normal fault had sliced part of the Murdama sediments that once covered
6
7 the Kirsh area and moved it westward. This model would establish a
8
9 situation where the ductile interior of the Kirsh dome is surrounded by a
10
11 brittle domain made up of the unmetamorphosed Jibalah sediments and
12
13 the slightly (lower greenschist facies) metamorphosed Murdama
14
15 molasses, with a detachment fault separating the two domains in a
16
17 manner identical to that of typical Phanerozoic core complexes.
18
19
20
21
22
23
24

25 Deep burial of the Kirsh paragneisses during continental collision
26
27 and the ensuing crustal thickening is evident from their high-P
28
29 mineralogy; similar deep crustal rocks were reported from gneiss domes
30
31 associated with major strike-slip systems with pressures reaching up to 12
32
33 kbars (e.g. Jolivet *et al*, 1999). Pressure estimates from Sinai complexes
34
35 are much lower being mainly in the range of 3–5.5 kbar with
36
37 temperatures of 500-650 °C (Brooijmans *et al*, 2003; Eliwa *et al*, 2008),
38
39 and thus define a relatively high geothermal gradient (30–50 °C/km) for a
40
41 collisional orogeny. Such a steep gradient and the LP/HT mineral
42
43 assemblages suggest that they were formed in an extensional setting with
44
45 heat flow transferred from nearby granitic intrusions (Eliwa *et al*, 2008).
46
47 This type of scenario is untenable for the Kirsh dome which appears to
48
49 have developed through a process not controlled by thermal relaxation;
50
51
52
53
54
55
56
57
58
59
60
61
62
63
64
65

1
2
3 similarly, models where continuous magma generation weakened the
4
5 crust leading to facilitation of lateral extrusion tectonics do not apply
6
7 (Fritz *et al*, 2002). However, recent evidence from the Feiran–Solaf
8
9 migmatite/gneiss complex in Sinai which is located within a northerly
10
11 segment of the Najd system indicates peak metamorphic conditions at
12
13 700–750 °C and 7–8 kbar with subsequent isothermal decompression to
14
15 4–5 kbar, followed by near isobaric cooling to 450 °C (Abu-Alam, and
16
17 Stuwe, 2009). The prograde path of migmatites from this particular
18
19 complex corresponds roughly to a geothermal gradient of 25-30 °C/km
20
21 and reaches down to a depth of 25-29 Km.
22
23
24
25
26
27

28 The Artawi Structural Window (ASW) which is roughly coeval
29
30 with the Kirsh dome and occupy a similar structural setting (a dilational
31
32 segment of a Najd fault) has a clockwise P-T t path indicating thickening
33
34 prior to extensive heating, and with a relatively low geothermal gradient
35
36 for the prograde path averaging about 20 °C/km (Al-Saleh *et al*, 1998),
37
38 thus intersecting the wet granite solidus at a depth of approximately 30
39
40 Km (Thompson, 1999). The high variance assemblage of the Kirsh rocks
41
42 precludes the use of conventional thermobarometric techniques; however,
43
44 if the same conditions from the ASW apply to the Kirsh dome then the
45
46 entire prograde path would be within the kyanite stability field and
47
48 intersection with the granite solidus and the muscovite dehydration-
49
50 melting line (Thompson, 2001) would be attainable in the lower crust. A
51
52
53
54
55
56
57
58
59
60
61
62
63
64
65

1 more plausible scenario would be that dilation within the Rika Fault
2 induced substantial decompression that led to the intersection with
3 dehydration solidi at mid-crustal levels. This situation is commonly
4 recorded by migmatites in gneiss domes, and the typical magnitude of
5 decompression is at least 4–6 kbar (Teyssier and Whitney, 2002). As the
6 rocks decompress further and with a slight increase in temperature due to
7 the onset of thermal relaxation they would cross the biotite dehydration-
8 melting curve (Fig-5) beyond which a greater degree of melt is produced
9 (Vielzeuf and Holloway, 1988).

10
11
12
13
14
15
16
17
18
19
20
21
22
23
24
25
26
27
28
29
30
31
32
33
34
35
36
37
38
39
40
41
42
43
44
45
46
47
48
49
50
51
52
53
54
55
56
57
58
59
60
61
62
63
64
65

Extensional segments of regional strike-slip shear zones are favorable sites for the production and ascent of granitic magma, which may form by a combination of decompression-dehydration melting, and then infiltrate the shear zone at extensional jogs to be later squeezed upwards in zones of compression through the mechanism of strike slip dilatancy pumping (Brown, 1994). The Kirsh dome is situated within a major extensional offset of the Rika Fault that could have produced the necessary decompression and the ensuing dehydration melting through the reactivation of the thrust on its western boundary as a low-angle normal fault.

According to Clemens (1984) most granitic magmas were initially water-undersaturated, indicating that melting reactions were fluid-absent; and even if water-saturated melting was to occur a smaller fraction of

1 melt (>10%) is produced, and would be exceedingly difficult to segregate
2
3 into a mobile mass. A higher degree of melting (c. 40%) is attained by the
4
5 breakdown of hydrous phases, especially micas (Vielzeuf and Holloway,
6
7 1988); the positive slopes of these dehydration-melting solidi allow
8
9 intersection with even a near-isothermal decompression path (Fig-5), and
10
11 the resulting melt would then begin to flow into dilatant zones or move
12
13 upward diapirically due to density contrast, a process that would lead to
14
15 more isothermal decompression and which would halt solidification until
16
17 the migmatite-granite mass is emplaced within the upper crust where it
18
19 becomes subjected to rapid cooling. According to Teyssier and Whitney
20
21 (2002) the signature of the rapid ascent of partially molten crust is a
22
23 gneiss dome cored by migmatite ± granite which is similar to the situation
24
25 in the Kirsh dome. In their reviews of core complexes in the eastern
26
27 desert of Egypt Fritz *et al* (1996) and Fritz *et al* (2002) conclude that
28
29 although a regime of overall convergence and transpression prevailed,
30
31 displacement partitioning allowed overall orogen-parallel extension
32
33 during a bulk compressive regime. It is proposed here that the Kirsh
34
35 dome with its granitic core represents a metamorphic core complex
36
37 generated and exhumed by localized extension along a major releasing
38
39 bend of the Rika Fault following a major transpressional orogeny in the
40
41 eastern Arabian Shield.
42
43
44
45
46
47
48
49
50
51
52
53
54
55
56
57
58
59
60
61
62
63
64
65

1
2
3
4 **References:**
5
6
7

8 Abd El-Wahed MA (2008) Thrusting and transpressional shearing in
9
10 the Pan-African nappe southwest El-Sibai core complex, Central Eastern
11
12 Desert, Egypt. *J Afr Earth Sci* 50:16–36
13
14

15
16 Abd El-Wahed, M; in press; The role of the Najd Fault System in the
17
18 tectonic evolution of the Hammamat molasse sediments, Eastern Desert,
19
20 Egypt; *Arabian Journal of Geosciences*.
21
22

23
24 Abu-Alam, T S. and Stuwe, K., 2009, Exhumation during oblique
25
26 transpression: The Feiran-Solaf region, Egypt, *Journal of Metamorphic*
27
28 *Geology*, vol.27 no.6, 439-460.
29
30

31
32 Agar, R.A., 1985, Stratigraphy and paleogeography of the Siham
33
34 group: direct evidence for a late Proterozoic continental microplate and
35
36 active continental margin: *Journal of the Geological Society, London*, v.
37
38 142, p. 1205-1220.
39
40

41
42 Ali BH, Wilde SA, Gabr MMA (2009). Granitoid evolution in Sinai,
43
44 Egypt, based on precise SHRIMP U-Pb zircon geochronology. *Gondwana*
45
46 *Research*, 15, 38-48.
47
48

49
50 Al-Saleh A.M.; Boyle A.P.; Mussett A.E 1998. Metamorphism and
51
52 $^{40}\text{Ar}/^{39}\text{Ar}$ dating of the Halaban Ophiolite and associated units: evidence
53
54
55
56
57
58
59
60
61
62
63
64
65

1
2
3 for two-stage orogenesis in the eastern Arabian Shield. Journal of the
4 Geological Society, Volume 155, Number 1, p. 165-175 (11).

5
6 Andresen A, Abu El-Rus MA, Myhre PI, Boghdady GY, Corfu F
7
8 (2009) U–Pb TIMS age constraints on the evolution of the
9 Neoproterozoic Meatiq Gneiss dome, Eastern Desert, Egypt. Int J Earth
10 Sci, 98, 481-497.

11
12 Blasband, B., White, S., Brooijmans, P., Dirks, P., de Boorder, and
13 Visser, W., 2000. Late Proterozoic extensional collapse in the Arabian
14 Nubian Shield. Journal of the Geological Society, 157, 615-628.

15
16 Brooijmans, P.; Blasband, B.; White, S.H.; Visser, W.J., Dirks, P.
17 (2003): Geothermobarometric evidence for a metamorphic core complex
18 in Sinai, Egypt. *Precambrian Res.*, 123(2-4): 249-268.

19
20 Brown, M. 1994. The generation, segregation, ascent and
21 emplacement of granite magma: the migmatite-to-crustally-derived
22 granite connection in thickened orogens. *Earth-Science Reviews*, **36**(1–
23 2): 83–130.

24
25 Brown, G.F., Schmidt, D.L., Huffman, A.C., Jr., 1989. Geology of
26 the Arabian Peninsula. Shield Area of Western Saudi Arabia. U.S.
27 Geological Survey Professional Paper 560-A, p. 188.

28
29 Calvez, J. Y., Alsac, C., Delfour, J., Kemp, J., Pellaton, C. (1983) -
30 Geologic evolution of the western, central and eastern parts of the
31
32
33
34
35
36
37
38
39
40
41
42
43
44
45
46
47
48
49
50
51
52
53
54
55
56
57
58
59
60
61
62
63
64
65

1 Northern Precambrian Shield, Kingdom of Saudi Arabia. Directorate
2
3 General of Mineral Resources, open file report BRGM, OF-03-17.
4

5 Clemens, J.D. (1984) water contents of silicic to intermediate
6
7
8
9
10
11
12
13
14
15
16
17
18
19
20
21
22
23
24
25
26
27
28
29
30
31
32
33
34
35
36
37
38
39
40
41
42
43
44
45
46
47
48
49
50
51
52
53
54
55
56
57
58
59
60
61
62
63
64
65

Clemens, J.D. (1984) water contents of silicic to intermediate
magmas. *Lithos*, 17, 273-287.

Collenette, P., Grainger, D.J., 1994, Mineral Resources of Saudi
Arabia, DGMR Special Publication SP-2.

Delfour, J., 1979. Geologic Map of the Halaban quadrangle, sheet
23G, Kingdom of Saudi Arabia. Saudi Arabian Deputy Ministry For
Mineral Resources Geoscience Map GM 46C, scale 1:250 000, with text,
32 p.

Delfour, J., 1980. Geologic Map of the Ar Rika quadrangle, sheet
22G, Kingdom of Saudi Arabia. Saudi Arabian Deputy Ministry For
Mineral Resources Geoscience Map GM 51A, scale 1:250 000, with text,
34 p.

D'Lemos, R.S., Brown, M. and Strachan, R.A., 1992. Granite
magma generation, ascent and emplacement within a transpressional
orogen. *Geological Society of London. Journal*, 149:487-490.

Eliwa, H. A.; Abu El-Enen, M. M.; Khalaf, I. M.; Itaya, T.; Murata,
M.; 2008, Metamorphic evolution of Neoproterozoic metapelites and
gneisses in the Sinai, Egypt: Insights from petrology, mineral chemistry
and K–Ar age dating *Journal of African Earth Sciences*, v. 51, iss. 3, p.
107-122.

1 Fowler, A., El-Kalioubi, B., 2002. The Migif-Hafafit gneissic
2 complex of the Egyptian Eastern Desert: fold interference patterns
3 involving multiply deformed sheath folds. *Tectonophysics* 346, 247–275.
4
5
6

7
8 Fowler, A; Hassan, I; 2008; Extensional tectonic origin of
9 gneissosity and related structures of the Feiran-Solaf metamorphic belt,
10 Sinai, Egypt *Precambrian Research* Volume: 164 Issue: 3-4 Pages:
11 119-136 .
12
13
14
15
16
17
18

19
20 Fowler, A., Khamees, H., Dowidar, H., 2007. El-Sibai Gneissic
21 Complex, Central Eastern Desert, Egypt: folded nappes and synkinematic
22 gneissic granitoid sheets – not a core complex. *J. Afr. Earth Sci.* 49, 119-
23 135.
24
25
26
27
28
29
30

31 Fritz, H., Dallmeyer, D.R., Wallbrecher, E., Loizenbauer, J.,
32 Hoinkes, G., Neumayr, P., Khudeir, A.A., 2002. Neoproterozoic
33 tectonothermal evolution of the Central Eastern Desert, Egypt: a slow
34 velocity tectonic process of core complex exhumation. *Journal of African*
35 *Earth Sciences* 34, 137–155.
36
37
38
39
40
41
42
43
44

45 Fritz, H., Wallbrecher, E., Khudeir, A.A., Abu El Ela, F. and
46 Dallmeyer, R.D., 1996, Formation of Neoproterozoic metamorphic core
47 complexes during oblique convergence: Eastern Desert, Egypt: *Journal of*
48 *African Earth Sciences*, v. 23, p. 311-329.
49
50
51
52
53
54
55
56
57
58
59
60
61
62
63
64
65

1 Genna, A., Nehlig, P., Le Goff, E., Guerrot, C., and Shanti, M.,
2
3 2002. Proterozoic tectonism of the Arabian Shield: Precambrian
4
5 Research, v. 117, p. 21-40.
6

7
8 Hodges, K. V. (1991). Pressure–temperature–time paths. Annual
9
10 Review of Earth and Planetary Sciences, 19:207–236.
11

12
13 Johnson, P.R., 1998, Tectonic map of Saudi Arabia and adjacent
14
15 areas: Saudi Arabian Deputy Ministry for Mineral Resources Technical
16
17 Report USGS-TR-98-3, scale 1:4,000,000.
18
19

20
21 Johnson, P.R. 2000. Proterozoic geology of Saudi Arabia: current
22
23 concepts and issues. Workshop on the Geology of the Arabian Peninsula,
24
25 6th Meeting of the Saudi Society for Earth Science. King Abdulaziz City
26
27 for Science & Technology, Riyadh, 1–32.
28
29

30
31 Johnson, P.R., 2003, Post-amalgamation basins of the NE Arabian
32
33 shield and implications for Ediacaran tectonism in the northern East
34
35 African orogen: Precambrian Research, v. 123, p. 321-337.
36
37

38
39 Johnson, P.R., 2005, Proterozoic geology of western Saudi Arabia,
40
41 east-central sheet (revised, digital edition): Saudi Geological Survey
42
43 Open-File Report SGS-OF-2004-9, 48 p.
44
45

46
47 Johnson, P.R., 2006a, Digital map of Proterozoic rocks in western
48
49 Saudi Arabia: Meta-data. Saudi Geological Survey Data-File Report
50
51 SGS-DF-2005-7.
52
53
54
55
56
57
58
59
60
61
62
63
64
65

1 Johnson, P.R., 2006b, Explanatory notes to the map of Proterozoic
2 geology of western Saudi Arabia: Saudi Geological Survey Technical
3 Report SGS-TR-2006-4, 62 p., 22 figs., 2 plates.
4
5
6
7

8 Johnson, P.R., and Kattan, F., 1998, The Ruwah, Ar Rika, and
9 Halaban-Zarghat fault zones: northwest-trending Neoproterozoic brittle-
10 ductile shear zones in west-central Saudi Arabia, in H. De Wall and R.O.
11 Greiling (editors) Aspects of Pan-African Tectonics Proceedings of a
12 discussion meeting at Heidelberg, October 1998, Series International
13 Cooperation, Bilateral Seminars, Forschungszentrum.
14
15
16
17
18
19
20
21
22
23
24

25 Johnson, P.R. and Woldehaimanot, B., 2003. Development of the
26 Arabian-Nubian Shield: perspectives on accretion and deformation in the
27 northern East African Orogen and the assembly of Gondwana. In:
28 Proterozoic East Gondwana: Supercontinent Assembly and Breakup (eds.
29 Yoshida, M., Windley, B.F. and Dasgupta S.). *Geological Society,*
30 *London, Spec. Publ.*, 206, 289-325.
31
32
33
34
35
36
37
38
39
40
41

42 Jolivet L., Maluski H., Beyssac O., Goffe B., Lepvrier C., Thi P.T.
43 and Nguyen V.V. (1999) Oligocene-Miocene Bu Khang extensional
44 gneiss dome in Vietnam: Geodynamic implications, *Geology*, 27, 1, 67-
45
46
47
48
49
50
51 70.
52

53 Kroner, A., Roobol, M.J., Ramsay, C.R., Jackson, N.J., 1979. Pan
54 African ages of some gneissic rocks in the Saudi Arabian Shield. *Journal*
55 *of the Geological Society of London* 136, 455– 461.
56
57
58
59
60
61

1
2
3
4
5
6
7
8
9
10
11
12
13
14
15
16
17
18
19
20
21
22
23
24
25
26
27
28
29
30
31
32
33
34
35
36
37
38
39
40
41
42
43
44
45
46
47
48
49
50
51
52
53
54
55
56
57
58
59
60
61
62
63
64
65

Loizenbauer, J., Wallbrecher, E., Fritz, H., Neumayr, P., Khudier, A.A., Kloetzli, U. (2001): Structural geology, single zircon ages and fluid inclusion studies of the Meatiq metamorphic core complex: Implications for Neoproterozoic tectonics in the Eastern Desert of Egypt, *Precambrian Research* 110, pp 357 – 383.

Matsah, M.I., 2000. The deposition of the Jibalah Group in pull-apart basins of the Najd Fault System as a final stage of the consolidation of Gondwanaland, Ph.D. thesis, *Boston University*, Boston, Massachusetts, U.S.A. 333p.

Matsah, M.I., Kusky, T., 2001. Analysis of Landsat TM ratio imagery of the Halaban-Zarghat fault and related Jifn basin, NE Arabian Shield: implications for the kinematic history of the Najd fault system. *Gondwana Res.* 4, 182 (abstract).

Miller, N.R., Johnson, P.R., Stern, R.J., 2008. Marine versus non-marine environments for the Jibalah group, NW Arabian shield: A sedimentologic and geochemical survey and report of possible metazoa in the Dhaiqa formation. *Arabian Journal for Science and Engineering* Theme Issue: Arabian Plate Basement Rocks and Mineral Deposits, 33, 1C, 55-77.

Mogren, S., Al-Amri, A. M., Al-Damegh, K., Fairhead, D., Jassim, S. and A. Algamdi, 2008, Sub-surface geometry of Ar Rika and Ruwah

1 faults from Gravity and Magnetic Surveys, Arabian Journal of
2 Geosciences, 1:33–47.
3

4
5 Nehlig, P; Asfirane, F; Genna, A; Guerrot, C; Nicol, N; Salpeteur, I;
6
7 Shanti, M; Thiéblemont, D; 2001; Aeromagnetic map constrains
8
9 cratonization of the Arabian Shield; Terra Nova, Volume 13, Number 5,
10
11 pp. 347-353(7).
12
13

14
15
16 Nehlig P., Genna A., Asfirane F., Dubreuil N., Guerrot C., Eberlé,
17
18 J.M, Kluyver H.M., Lasserre J.L., Le Goff E., Nicol N., Salpeteur N.,
19
20 Shanti M., Thiéblemont D., Truffert C., 2002, A review of the Pan-
21
22 African evolution of the Arabian Shield, Geoarabia, Vol. 7, No. 1.
23
24
25

26
27
28 Neumayr, P., Hoinkes, G., Puhl, J., Mogessie, A., Khudier, A.A.,
29
30 1998. The Meatiq dome (Eastern Desert, Egypt) a Precambrian
31
32 metamorphic core complex: petrological and geological evidence, Journal
33
34 of Metamorphic Geology 16, 259-279.
35
36
37

38
39
40 Ramsay, C.R., Jackson, N.J., Roobol, M.J. (1984)
41
42 Structural/lithological provinces in a Saudi Arabian Shield geotraverse.
43
44 In: Evolution and mineralization of the Arabian-Nubian SHield,
45
46 Proceedings Symposium 1-3 Feb., 1982, I.A.G. King Abdulaziz
47
48 University, Jeddah, Kingdom of Saudi Arabia, Tahoun, S.A.(ed.), p. 64-
49
50
51
52
53
54 84.
55

56
57 Schmidt, D.L. Hadley, D.G. and Stoesser, D.B. 1979. Late
58
59 Proterozoic crustal history of the Arabian Shield, southern Najd Province,
60
61

1 Kingdom of Saudi Arabia, Institute of Applied Geology Jeddah Bulletin,
2
3 3, 2, 41 58.
4

5 Shalaby, A., Stüwe, K., Fritz, H., Makroum, F. (2006): The El
6
7
8
9
10
11
12
13
14
15
16
17
18
19
20
21
22
23
24
25
26
27
28
29
30
31
32
33
34
35
36
37
38
39
40
41
42
43
44
45
46
47
48
49
50
51
52
53
54
55
56
57
58
59
60
61
62
63
64
65

Mayah molasse basin in the Eastern Desert of Egypt; Journal of African Earth Sciences 45, 1–15.

Stern, R.J. & Hedge, C.E. 1985. Geochronologic and isotopic constraints on Late Precambrian crustal evolution in the Eastern Desert of Egypt. American Journal of Science, 285, 97–127

Stoeser D.B. and Stacey J.S., 1988. Evolution, U-Pb geochronology and isotope geology of the Pan-African Nabitah orogenic belt of the Saudi Arabian Shield. In S. El-Gaby and R.O. Greiling (editors), The Panafrican Belt of Northeast Africa and Adjacent Areas. Vieweg, Braunschweig, pp. 227-288.

Teyssier, C., and Whitney, D., 2002, Gneiss domes and orogeny: Geology, v. 30, p. 1139–1142.

Thompson, A. B. (1999) Some Time-Space Relationships for Crustal Melting and Granitic Intrusion at various depths. In: *Understanding Granites*: A. Castro, C. Fernandez and J-L Vigneresse (eds), *Geological Society of London*, Special Publication, v. 158, pp. 7 –25.

Thompson, A.B., 2001, *P-T* paths, H₂O recycling, and depth of crystallization for crustal melts, *Phys. Chem. of the Earth*. Vol, 26, No. 4-5, pp. 231-237.

1
2
3
4
5
6
7
8
9
10
11
12
13
14
15
16
17
18
19
20
21
22
23
24
25
26
27
28
29
30
31
32
33
34
35
36
37
38
39
40
41
42
43
44
45
46
47
48
49
50
51
52
53
54
55
56
57
58
59
60
61
62
63
64
65

Vielzeuf, D. and Holloway, 1988. Experimental determination of the fluid-absent melting reactions in the pelitic system. Consequences for crustal differentiation. *Contributions to Mineralogy and Petrology* 98, 257-276.

Whitney, D.L., Teyssier, C., and Vanderhaeghe, O. (2004) Gneiss domes and crustal flow. In: Whitney, D.L., Teyssier, C., and Siddoway, C.S., (eds.), *Gneiss Domes in Orogeny*, Geological Society of America Special Paper 380, 15-33.

Wilde, S.A., and Youssef, K. (2002) A re-evaluation of the origin and setting of the Late Precambrian Hammamat Group based on SHRIMP U-Pb dating of detrital zircons from Gebel Umm Tawat, North Eastern Desert, Egypt. *Journal of the Geological Society*, 159, 595-604.

Willis, K.M., Stern, R.J. & Clauer, N. 1988. Age and geochemistry of Late Precambrian sediments of the Hammamat Series from the Northeastern Desert of Egypt. *Precambrian Research*, 42, 173–187.

Yin, A. 1991. Mechanisms for the formation of domal and basinal detachment faults: a three-dimensional analysis. *J. Geophys. Res.*, 96, 14,577-14,594.

Yin, A., 2004. Gneiss domes and gneiss dome systems, In Whitney, D.L., Teyssier, C., and Siddoway, C.S., eds., *Gneiss domes in orogeny*, Boulder Colorado, Geological Society of America Special Paper 380, p. 1-14.

1
2
3
4
5
6
7
8
9
10
11
12
13
14
15
16
17
18
19
20
21
22
23
24
25
26
27
28
29
30
31
32
33
34
35
36
37
38
39
40
41
42
43
44
45
46
47
48
49
50
51
52
53
54
55
56
57
58
59
60
61
62
63
64
65

Figures

Fig-1: Terrane map of the Arabian Shield showing the main segments of the Najd Fault System and their associated gneissic domains (from Johnson, 2006b).

Fig-2: Simplified geologic map of the northernmost part of the Kirsh Dome (after Delfour, 1979 & 1980; Johnson, 2003). Due to the left-stepping nature of the Rika Fault in this region the main fault line marks the western border of the dome while the northern contact with the Murdama sediments is more or less intrusive. The grey area marked (ky) is the main belt of kyanite-bearing quartzites.

1
2
3 Fig-3: Lower hemisphere stereoplot of mineral lineations in the
4 metamorphic mantle of the Kirsh Dome.

5
6 Fig-4: $^{39}\text{Ar}/^{36}\text{Ar}$ - $^{40}\text{Ar}/^{36}\text{Ar}$ normal isochron diagram of a biotite separate
7
8 from a paragneiss showing the errors at the 2σ level and a best-fit
9
10 regression line.

11
12
13 Fig-5: Postulated P-T-t path for the Kirsh migmatites (dashed bold line)
14 showing the location of the wet granite solidus (WGS) and the
15
16 dehydration solidi for muscovite (MDS) and biotite (BDS). A
17
18 combination of dehydration melting and unroofing could have led to
19
20 isothermal decompression. P-T-t path from the ASW (Al-Saleh *et al*,
21
22 1998), Meatiq Dome = Md (Neumayr *et al.*, 1998) and the Feiran-Solaf
23
24 core complex = FS (Abu-Alam, and Stuwe, 2009) were added for
25
26 comparison, and they define a metamorphic field gradient of about $30^\circ\text{C}/$
27
28 km. A distinct decrease in the depth of burial/exhumation for the last two
29
30 regions might indicate a diminishing depth for the Najd system in the
31
32 northern Nubian Shield.
33
34
35
36
37
38
39
40
41
42
43
44
45
46
47
48
49
50
51
52
53
54
55
56
57
58
59
60
61
62
63
64
65

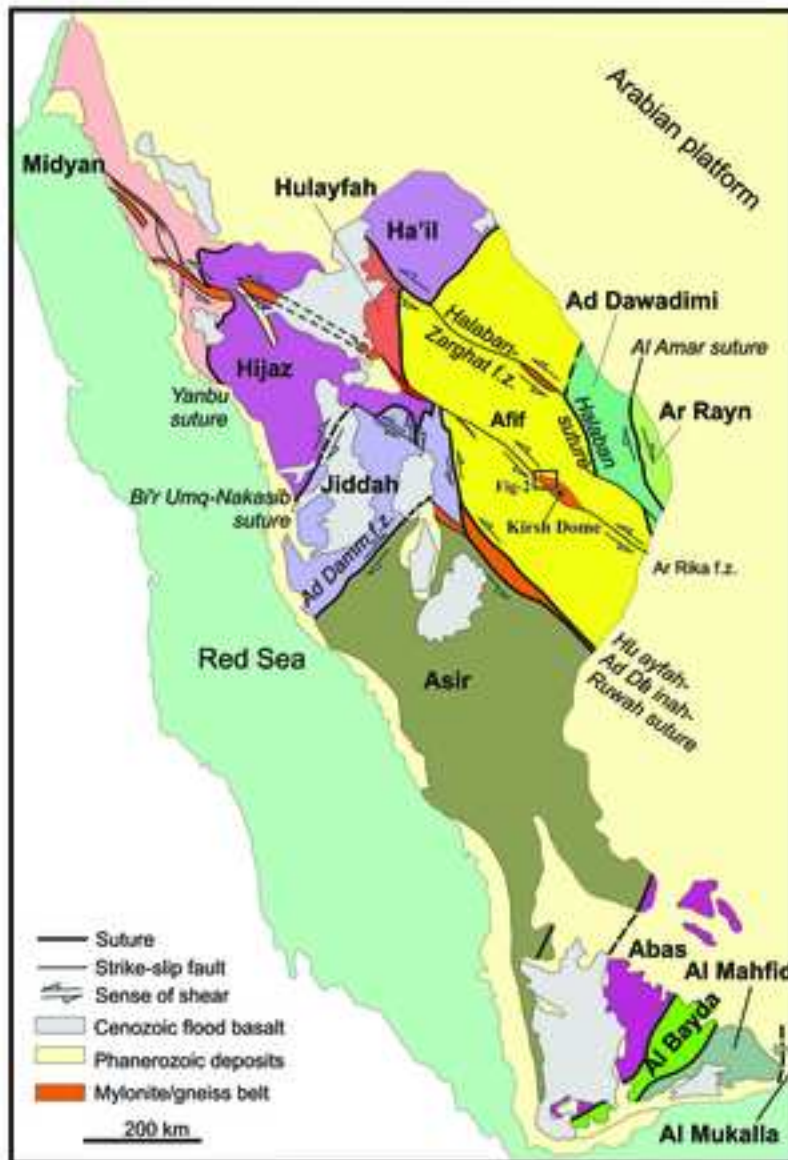
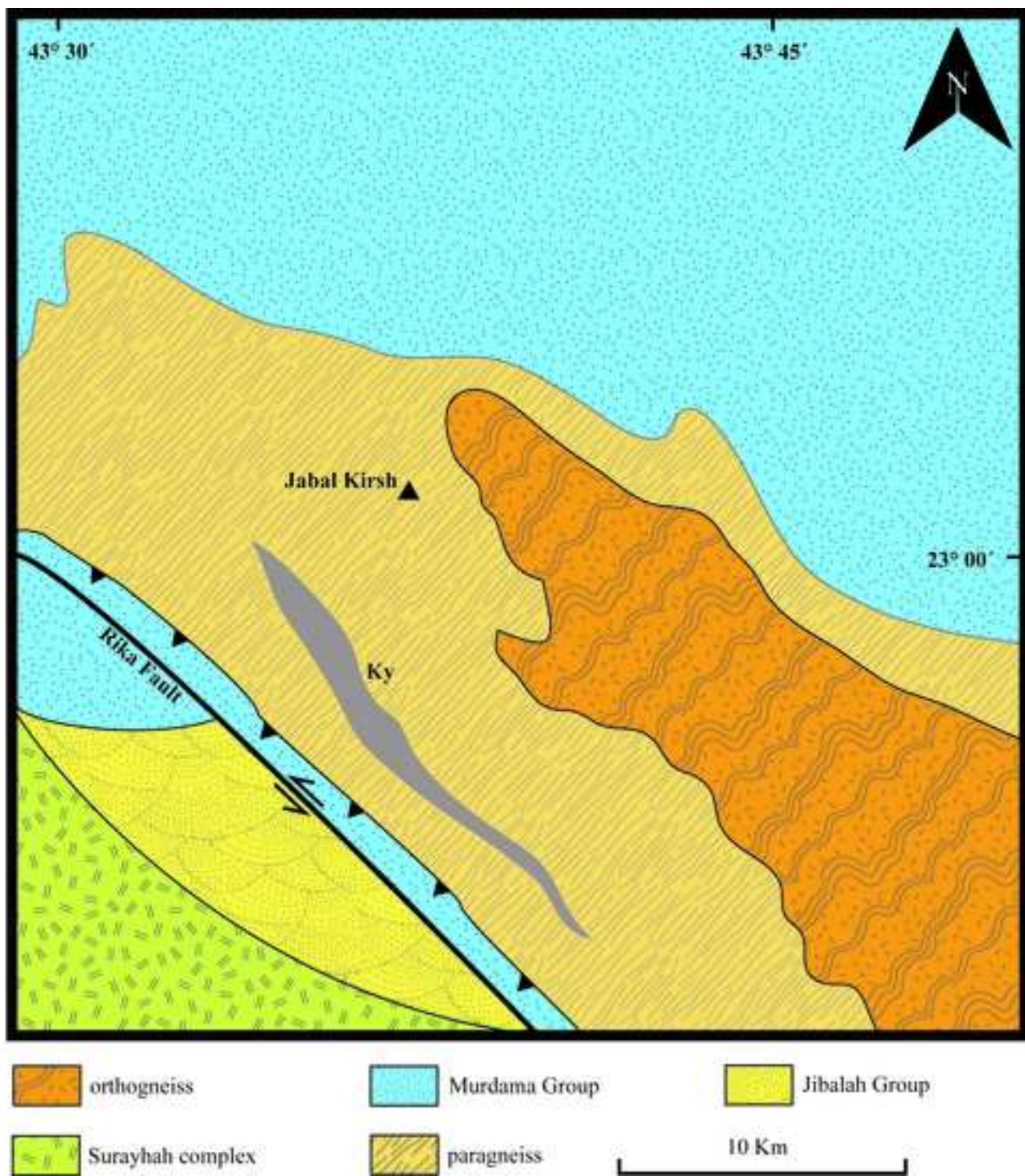


Fig -1

Figure
[Click here to download high resolution image](#)



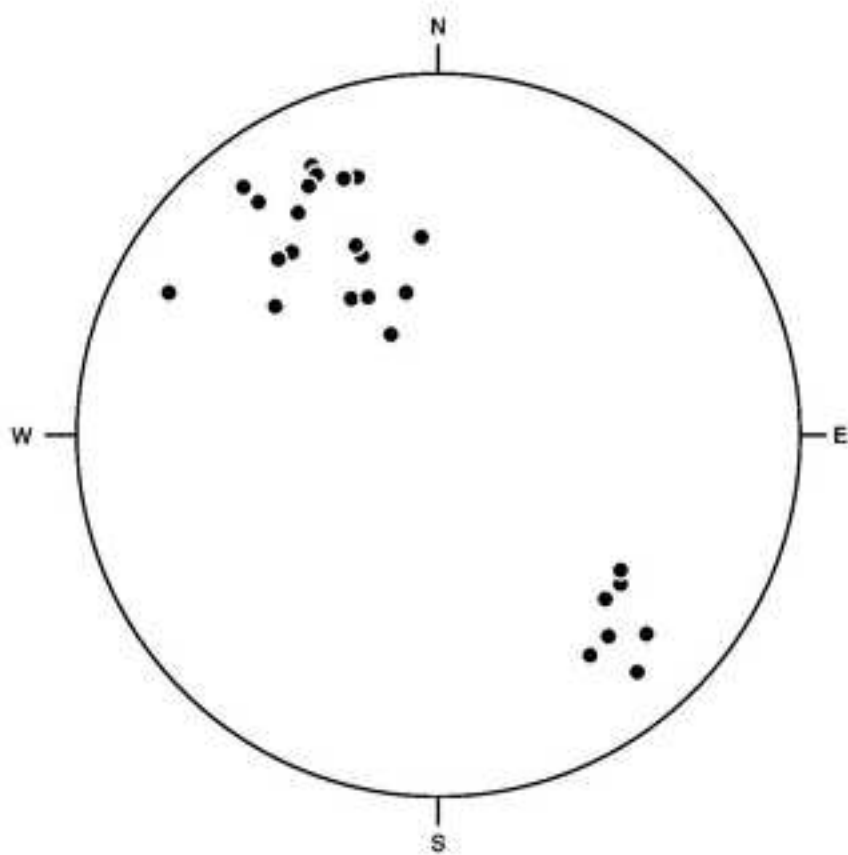


Fig-3

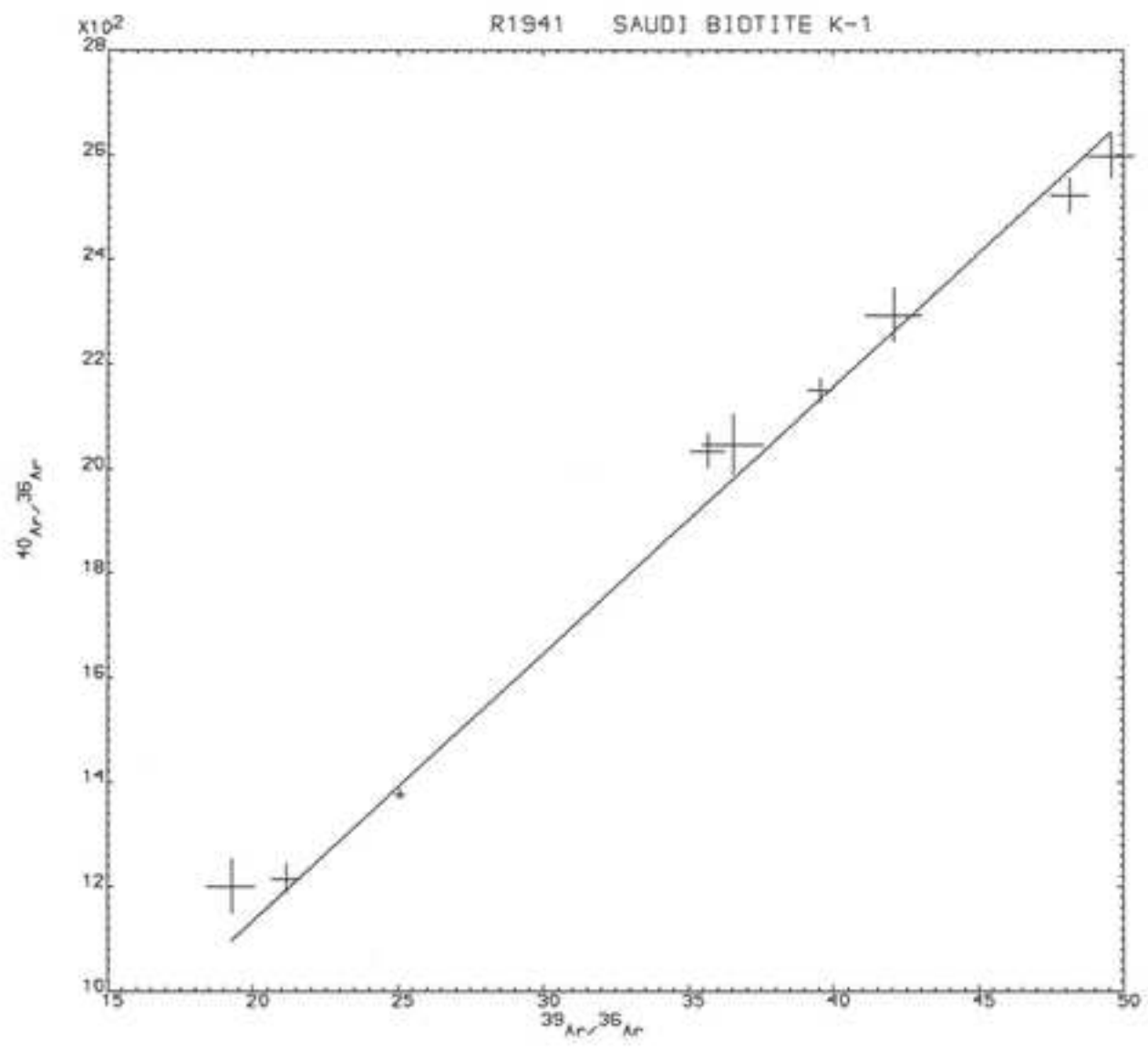


Fig-4

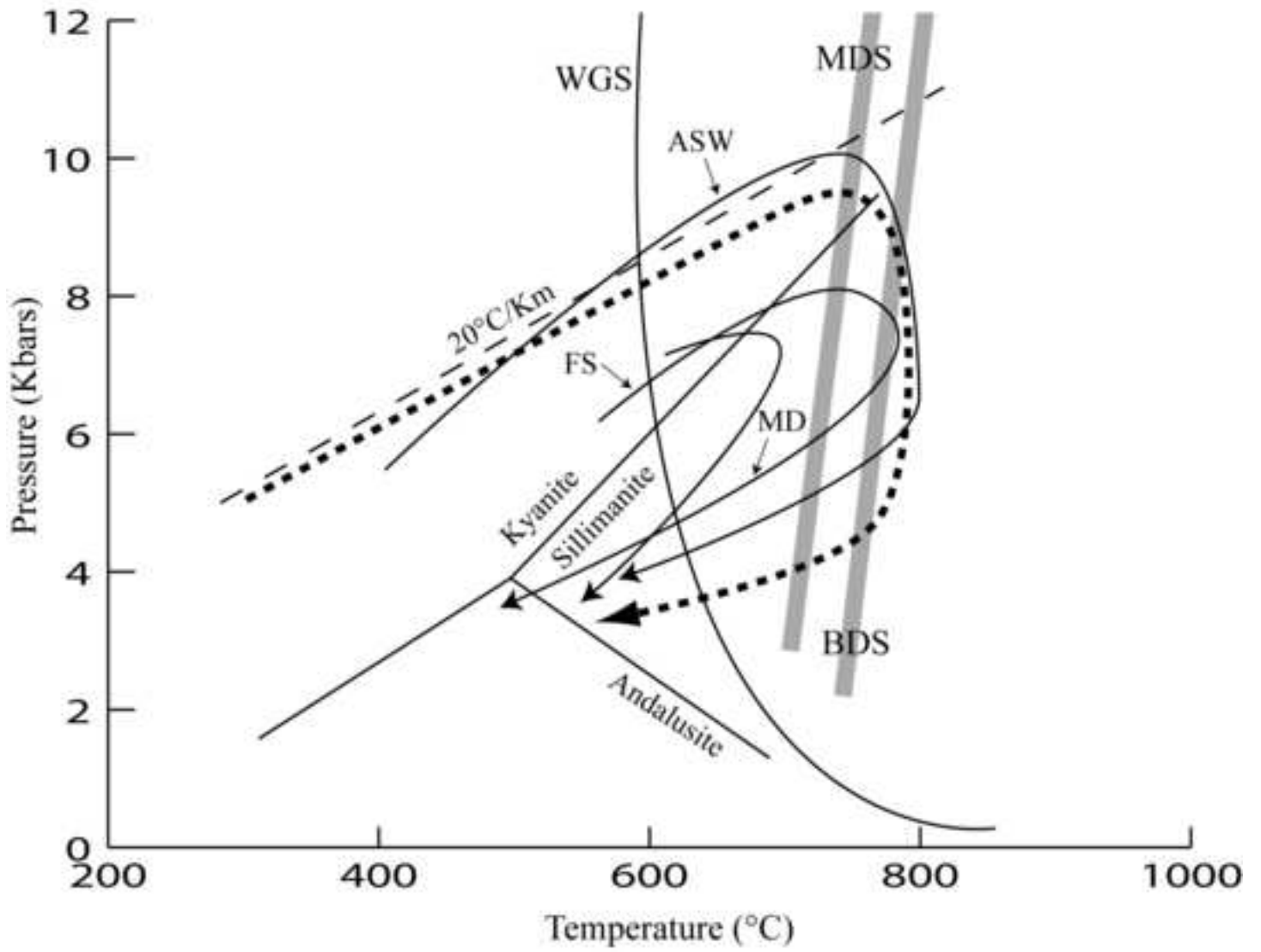


Fig-5